

Brillouin gain spectrum characterization in Ge-doped large-mode-area fibers

Xia-Xia Niu(牛夏夏), Yi-Feng Yang(杨依枫), Zhao Quan(全昭), Chun-Lei Yu(于春雷), Qin-Ling Zhou(周秦岭), Hui Shen(沈辉), Bing He(何兵), and Jun Zhou(周军)

Citation: Chin. Phys. B, 2021, 30 (**12**): 124203. DOI: 10.1088/1674-1056/abf7ab
Journal homepage: http://cpb.iphy.ac.cn; http://iopscience.iop.org/cpb

What follows is a list of articles you may be interested in

A low-threshold multiwavelength Brillouin fiber laser with double-frequency spacing based on a small-core fiber

Lu-Lu Xu(徐路路), Ying-Ying Wang(王莹莹), Li Jiang(江丽), Pei-Long Yang(杨佩龙), Lei Zhang(张磊), and Shi-Xun Dai(戴世勋)

Chin. Phys. B, 2021, 30 (**8**): 084210. DOI: 10.1088/1674-1056/abff47

Distributed analysis of forward stimulated Brillouin scattering for acoustic impedance sensing by extraction of a 2nd-order local spectrum

Yu-Lian Yang(杨玉莲), Jia-Bing Lin(林佳兵), Li-Ming Liu(刘黎明), Xin-Hong Jia(贾新鸿), Wen-Yan Liang(梁文燕), Shi-Rong Xu(许世蓉), and Li Jiang(姜利)

Chin. Phys. B, 2021, 30 (**8**): 084205. DOI: 10.1088/1674-1056/abfcce

All-fiberized very-large-mode-area Yb-doped fiber based high-peak-power narrow-linewidth nanosecond amplifier with tunable pulse width and repetition rate

Min Yang(杨敏), Ping-Xue Li(李平雪), Dong-Sheng Wang(王东生), Ke-Xin Yu(于可新), Xue-Yan Dong(董雪岩), Ting-Ting Wang(王婷婷), Chuan-Fei Yao(姚传飞), and Wei-Xin Yang(杨卫鑫)

Chin. Phys. B, 2020, 29 (**11**): 114206. DOI: 10.1088/1674-1056/abb3e9

Polarization dependence of gain and amplified spontaneous Brillouin scattering noise analysis for fiber Brillouin amplifier

Kuan-Lin Mu(穆宽林), Jian-Ming Shang(商建明), Li-Hua Tang(唐丽华), Zheng-Kang Wang(王正康), Song Yu(喻松), Yao-Jun Qiao(乔耀军)

Chin. Phys. B, 2019, 28 (**9**): 094216. DOI: 10.1088/1674-1056/ab38ab

High-gain and low-distortion Brillouin amplification based on pump multi-frequency intensity modulation

Li-Wen Sheng(盛立文), De-Xin Ba(巴德欣), Zhi-Wei Lv(吕志伟)

Chin. Phys. B, 2019, 28 (**2**): 024212. DOI: 10.1088/1674-1056/28/2/024212

Brillouin gain spectrum characterization in Ge-doped large-mode-area fibers*

Xia-Xia Niu(牛夏夏)[1,2], Yi-Feng Yang(杨依枫)[1,†], Zhao Quan(全昭)[1], Chun-Lei Yu(于春雷)[1], Qin-Ling Zhou(周秦岭)[1], Hui Shen(沈辉)[1], Bing He(何兵)[1,‡], and Jun Zhou(周军)[1]

[1] *Shanghai Key Laboratory of All Solid-State Laser and Applied Techniques, Shanghai Institute of Optics and Fine Mechanics, Chinese Academy of Sciences, Shanghai* 201800, *China*

[2] *Center of Materials Science and Optoelectronics Engineering, University of Chinese Academy of Sciences, Beijing* 100049, *China*

(Received 24 February 2021; revised manuscript received 12 April 2021; accepted manuscript online 14 April 2021)

The dependence of Brillouin gain spectrum (BGS) characteristics, including the Brillouin frequency shift (BFS) and the BGS bandwidth, on germanium concentration in large-mode-area Ge-doped passive fibers is investigated theoretically and experimentally. The simulation results show that the BFS is inversely proportional to GeO_2 concentration, and the BGS bandwidth initially increases with the augment of GeO_2 concentration, and then decreases. The BGSs of four fibers with core diameters of 10 μm and 20 μm for different GeO_2 concentrations are compared experimentally. Experimental results demonstrate that with the same core diameter, the variations of BFS and BGS bandwidths with GeO_2 concentration accord with the simulation results. Additionally, the BGS characteristics of three large-mode-area passive fibers with diameters of 10 μm, 25 μm, and 30 μm are measured, which confirm that the increasing of the fiber diameters will cause the BGS bandwidth to broaden. We believe that these results can provide valuable references for modulating the high-power narrow-linewidth fiber lasers and Brillouin fiber amplifiers.

Keywords: stimulated Brillouin scattering, Brillouin gain spectrum, large-mode-area fibers, fiber laser

PACS: 42.55.Wd, 42.65.Es, 42.65.–k **DOI:** 10.1088/1674-1056/abf7ab

1. Introduction

The applications of high-power narrow-linewidth fiber lasers to coherent beam combining and spectral beam combining have attracted widespread attention in recent years.[1,2] Stimulated Brillouin scattering (SBS) is the most limiting effect in terms of power handling capacity in high-power narrow-linewidth fiber lasers.[3,4] Over the decades, a variety of techniques have been implemented in order to suppress SBS,[5] such as introducing nonuniformities by stressing the optical fiber,[6] reducing the overlap between the light wave field and the sound wave field in the core by changing the doping composition and distribution in the core,[7–10] reducing effective fiber length,[11] broadening spectral linewidth of seed by pure phase modulation, *etc*.[12–15] Specifically, white noise source (WNS)[16–19] and pseudo-random binary sequence (PRBS)[20–23] phase modulation become the leading linewidth broadening schemes for high power fiber amplifiers which are required to balance the narrow-linewidth and the output power. In the commonly used PRBS phase modulation scheme, the SBS suppression capability can be determined by the separation between the discrete adjacent sidebands lying within the envelope, which should be appreciably more than twice the Brillouin gain spectrum (BGS) bandwidth.[14] In this scenario, the BGS characteristics become essential for designing the PRBS phase modulation scheme.

As is well known, the core dimensions and GeO_2 concentration of the fibers can dramatically affect the BGS characteristics, especially the Brillouin frequency shift (BFS) and the BGS bandwidth. Some efforts have devoted to studying the BGS in single-mode fiber (SMF). Nikles *et al.* have studied the influence of germanium concentration on BFS and BGS bandwidths, and they found that the change between BFS and GeO_2 concentrations is −94 MHz/wt%, while the change between BGS bandwidth and GeO_2 concentration is 1.4 MHz/wt%.[24] Li *et al.* reported the BFS is reduced by ∼ 1 GHz and BGS bandwidth is increased by ∼ 2 MHz when the core diameter decreases from 8.8 μm to 3 μm.[25] It is noticed that the germanium concentration of the fiber with a core diameter of 8.8 μm in Ref. [25] is 4 wt%, while the germanium concentration of the fiber with a core diameter of 3 μm is 19 wt%, showing the germanium concentrations of the fibers with different core diameters are different, and the BFS with GeO_2 concentration is about −89 MHz/wt%.[26] Li *et al.* showed that core doping GeO_2 concentration has a greater influence on the BFS than the core diameter and reducing fiber core diameter will result in a wider BGS bandwidth.[25] The above

*Project supported by the Key-Area Research and Development Program of Guangdong Province, China (Grant No. 2018B090904001), the National Natural Science Foundation of China (Grant Nos. 61805261, 61405202, and 61705243), and the Youth Innovation Promotion Association, Chinese Academy of Sciences (Grant No. 2020252).

†Corresponding author. E-mail: yfyang@siom.ac.cn

‡Corresponding author. E-mail: bryanho@mail.siom.ac.cn

© 2021 Chinese Physical Society and IOP Publishing Ltd

results are based on the SMF reported. However, the dependence of BGS characteristics on the GeO_2 concentration and core diameter in large-mode-area (LMA) fibers have not yet been studied in detail.

The purpose of this work is to examine the relationship between the GeO_2 concentration and the Brillouin gain spectrum characteristics in the LMA fibers. We first numerically simulate the dependence of BFS and BGS bandwidths on GeO_2 concentration. Then we present the BGS bandwidth as a function of single-pass gain to explain the BGS bandwidth measured in this work under the condition of Brillouin gain narrowing. Moreover, the BGSs are experimentally characterized in four types of fibers with different GeO_2 concentrations and core diameters of 10 μm and 20 μm by using heterodyne detection method, indicating the dependence of BFS and BGS bandwidths on GeO_2 concentration under the same core diameter fiber. Finally, the BGSs of three fibers with core diameters of 10 μm, 25 μm, and 30 μm are tested to demonstrate the influence of the core diameter on the BGS bandwidth.

2. Theory

In the kinetics of spontaneous Brillouin scattering, the BGS line is Lorentzian according to the exponential decay of phonons.[27] In a fiber system, spectral density function of the Stokes radiation, $S(\omega)$,[28] can be defined as

$$S(\omega)=\frac{4h\omega_{\rm s}(N+1)}{ncA\Gamma_{\rm B}}\left[\exp\left(\frac{G(\Gamma_{\rm B}/2)^2}{\omega^2+(\Gamma_{\rm B}/2)^2}\right)-1\right], \quad (1)$$

where h is the Planck's constant, N is the mean number of phonons per mode of acoustic field, $\omega_{\rm s}$ is the Stokes frequency, A is the effective cross-section area, and $\Gamma_{\rm B}$ is the phonon intensity decay rate, ω is the laser frequency, n is the effective refractive index of the pump mode, c is the propagation speed of light in vacuum. G is the single-pass gain, which can be defined as

$$G=g_0L_{\rm eff}P/A_{\rm eff}, \quad (2)$$

where g_0 is the peak value of the Brillouin gain, $L_{\rm eff}$ is the effective length, $A_{\rm eff}$ is the effective cross-sectional area of the interaction region, and P is the incident laser power. The gain factor g can be defined as

$$g_0=\gamma_{\rm e}^2\omega^2/\rho_0nc^3\upsilon_{\rm A}\Gamma_{\rm B}, \quad (3)$$

where $\gamma_{\rm e}$ is the electrostrictive constant of silica, ρ_0 is the mass density, and $\upsilon_{\rm A}$ is the acoustic velocity. As shown in Eq. (1), the spectral shape of the Stokes light depends on the single-pass gain G and the phonon intensity decay rate $\Gamma_{\rm B}$. The BGS bandwidth $\Gamma=\Gamma_{\rm B}/(2\pi)$ is the full width at half maximum (FWHM) of the BGS, which can be expressed as

$$\frac{1}{\Gamma_{\rm B}}=\frac{10^{-6}}{2\pi(17.5+0.71\times\omega_{GeO_2})}. \quad (4)$$

According to Ref. [28], the refractive index n of the medium, the acoustic velocity $\upsilon_{\rm A}$, and the mass density ρ_0 vary with GeO_2 concentration $\omega_{\rm Ge}$ [in unit wt%] and F concentration $\omega_{\rm F}$ [in unit wt%] and can be expressed respectively as[29]

$$n(\omega_{\rm Ge},\omega_{\rm F}) = 1.458(1+1.0\times10^{-3}\omega_{GeO_2} -3.3\times10^{-3}\omega_{\rm F}), \quad (5)$$

$$\upsilon_{\rm A}(\omega_{\rm Ge},\omega_{\rm F}) = 5944(1-7.2\times10^{-3}\omega_{GeO_2} -2.7\times10^{-2}\omega_{\rm F}), \quad (6)$$

$$\rho_0(\omega_{\rm Ge},\omega_{\rm F}) = 2202(1+6.4\times10^{-3}\omega_{GeO_2} -3.4\times10^{-3}\omega_{\rm F}). \quad (7)$$

The BGS bandwidth $\Delta\nu$ narrows as single-pass gain increases, which can be given by[28,30]

$$\Delta\nu=\Gamma\left[\frac{\ln 2}{G}\right]^{1/2}. \quad (8)$$

For small G (such as $G<5$ Np), the shape of the Brillouin gain spectrum is Lorentzian curve with a bandwidth of $\Delta\nu=\Gamma$. On the other hand, the Stokes spectrum bandwidth has almost no obvious change for large G (such as $G>20$ Np).[31]

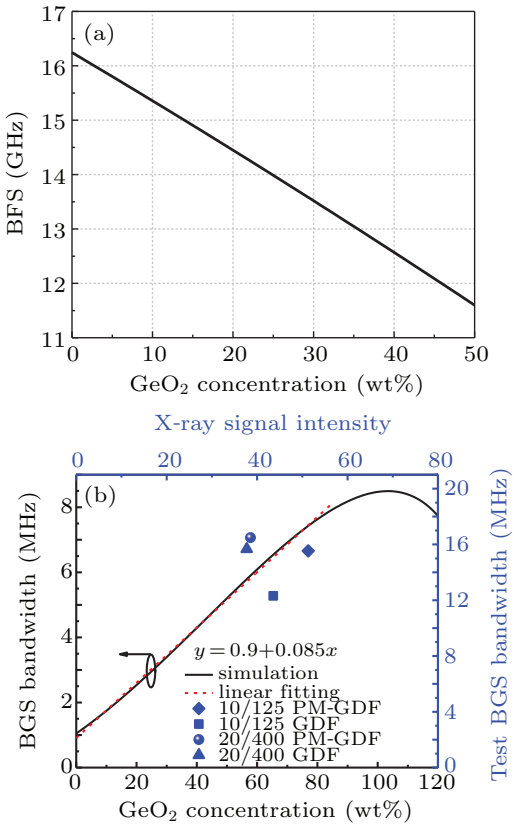


Fig. 1. (a) Simulated BFS *versus* GeO_2 concentration, and (b) calculated BGS bandwidth and tested bandwidth *versus* GeO_2 concentration for four types of fibers.

The generated Stokes frequency depends on the optical and acoustic properties of the propagation material as well as

the pump wavelength. The BFS in an LMA fiber can be defined as[32]

$$\nu_{\mathrm{B}} = \frac{2n\nu_{\mathrm{A}}}{\lambda}\cos(\theta/2), \tag{9}$$

where λ is the laser wavelength, and θ is the scattering angle of a mode. In the simulation, the influence of the scattering angle on the BFS is ignored. The BFS and BGS bandwidths as a function of GeO_2 concentration are shown in Figs. 1(a) and 1(b). The parameters and the values used in the simulation are shown in Table 1. Figure 1(a) shows that the BFS is inversely proportional to GeO_2 concentration and the relationship is linear. Figure 1(b) shows that the BGS bandwidth initially increases linearly and then decreases. The gain factor and single-pass gain will increase when the germanium concentration exceeds 80%, thus causing the narrowed Brillouin bandwidth to decrease. The red line is the linear fit with a slope of 0.085.

Table 1. Parameters and values used in simulation.

Parameters	Value	Parameters	Value
ω	1.77×10^{15} rad/s	γ_e	1.95
n	1.45	c	3×10^{8} m/s
λ	1067 nm		

The relationship between Brillouin gain factor g_0 and GeO_2 concentration is obtained by substituting Eqs. (4)–(7) into Eq. (3), and the results are shown in Fig. 2(a). It is demonstrated that as the GeO_2 concentration increases, Brillouin gain factor decreases initially, and then increases when the GeO_2 concertation exceeds 80%. Firstly, the phonon intensity attenuation rate, the refractive index, and the medium density increase faster than the sound velocity decreases, so the gain factor is reduced. With the increase of germanium concentration, the attenuation rate of the phonon intensity, the rate of increase of refractive index, and the medium density are lower than the rate of decrease of sound velocity, as a result, the gain factor has a minimum value, and then gradually increases. The single-pass gain dependence of BGS bandwidth can be obtained based on Eq. (8), and is plotted in Fig. 2(b). The results indicate that as the GeO_2 concentration increases, Brillouin gain factor initially decreases, and then increases. The Brillouin gain narrowing is shown in Fig. 2(b).

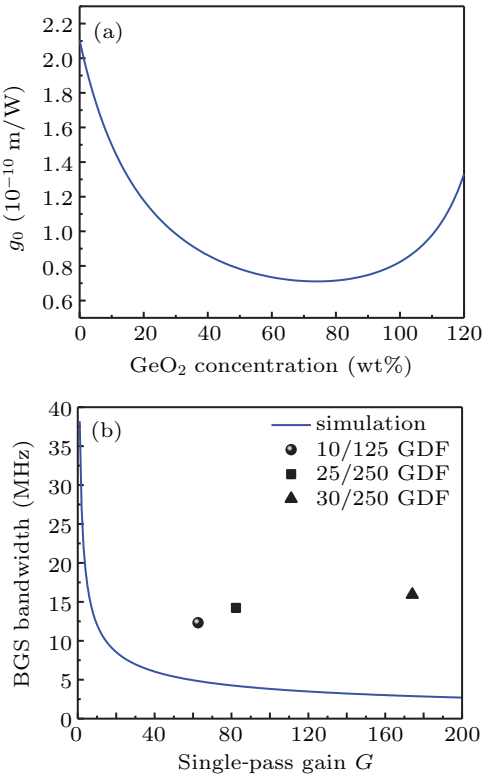


Fig. 2. (a) Simulated Brillouin gain factor *versus* GeO_2 concentration, and (b) calculated BGS bandwidth *versus* single-pass gain G and the experimental bandwidth of fibers with different core diameters.

3. Experimental setup

The BGSs of the LMA fibers are measured. The schematic diagram of the setup is shown in Fig. 3.

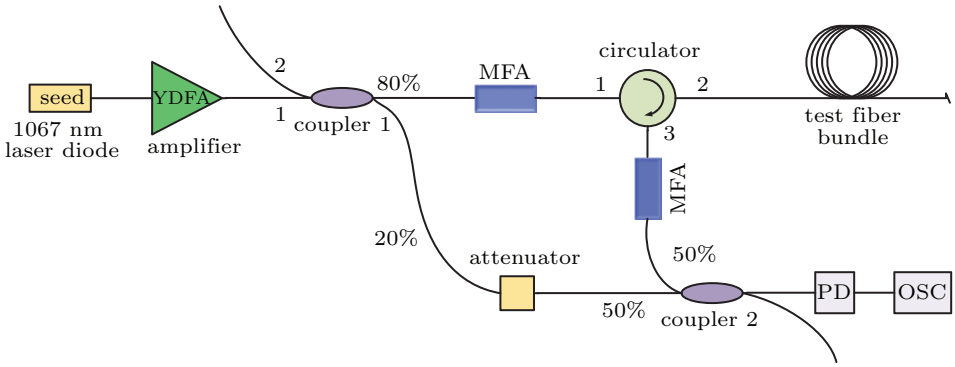


Fig. 3. Experimental setup of Brillouin gain spetrum measurement. MFA: mode field adapter; YDFA: Yb-doped fiber amplifier; PD: photodetector; RFA: radio frequency analyzer.

A 1067-nm, 60-mW, 3-kHz linewidth (the Rock, NP Photonics) single-frequency fiber laser is used as a light source. The laser signal is amplified to 10 W by a Yb-doped fiber amplifier (YDFA). The output laser is divided into two arms by an 80/20 coupler (coupler 1), where 80% of the laser pass through a circulator, and then connected to the input end of the

fiber under test (FUT). All the fibers are in a temperature range of 20 °C–22 °C and maintain the same bend radius to ensure the same experimental conditions. The generated backward Stokes light in the fiber is coupled into the 50/5 coupler (coupler 2) through port 3 of the circulator. The MFAs here is used to adapt the mode field. In the other arm, 20% of the laser acts as the reference light, and the power is controlled by an optical attenuator to maximize the visibility of the beat signal. The backward light and the reference light then beat in coupler 2, and the beat signal is detected by a photodetector (1014, Newport) with a maximum bandwidth of 46 GHz, and analyzed by a radio frequency analyzer (RFA, DSOX4024A, KEYSIGHT). The output end of the FUT is cleaved with 8° to prevent feedback.

4. Results and discussion

Six passive fibers (I–VI) are investigated in the experimental setup, of which the detailed parameters are listed in Table 2. The input laser power is the output power of the amplifier when the beat frequency output power is 1 mW. The values of single-pass gain G for all the FUTs are much larger than 25, which means that all the Brillouin bandwidths we tested are gain-narrowed.

Table 2. Experimental parameters and their values.

Parameter	Units	Fiber I	Fiber II	Fiber III	Fiber IV	Fiber V	Fiber VI
GDF		10/125-PM	10/125	20/400-PM	20/400	25/250	30/250
Length	m	96	50	36	147	65	42
Input laser power	W	0.96	1.7	5.44	1.32	4.14	18.42
NA		0.075	0.075	0.065	0.065	0.065	0.062
g_0	$\times 10^{-11}$ (m/W)	7.28	7.89	8.4	8.5	8.45	8.95
G		62.56	62.60	93.19	93.37	82.36	174.11

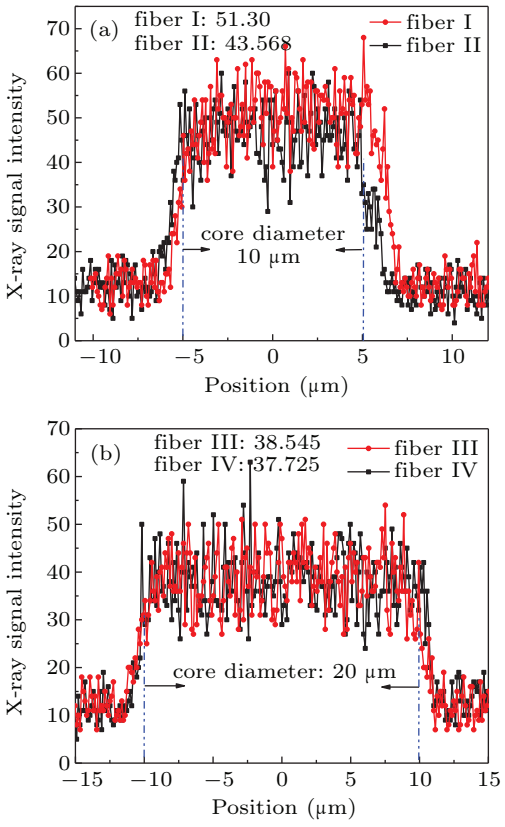


Fig. 4. X-ray signal intensity distribution for (a) fibers I and II and (b) fibers III and IV.

For comparing the core germanium concentrations of fibers with the same core diameter, we use the electron probe microanalysis (EPMA) to test the x-ray signal intensity of Ge doped in 10/125 and 20/400 polarization-maintaining and unpolarized fibers (fibers I–IV). The cross-sectional x-ray signal intensity distribution results for the four fibers are shown in Fig. 4. The x-ray signal intensity of each fiber is expressed by averaging the x-ray signal intensities in the core. The x-ray signal intensity can be used to characterize the germanium doping concentration because it is positively correlated with the content of GeO_2 in fiber. Figures 4(a) and 4(b) show that the germanium concentration of the polarization-maintaining fiber is higher than that of the unpolarized fiber, and the germanium concentration of the 10/125 fiber is higher than that of the 20/400 fiber.

The BFS and BGS bandwidths for fibers I–IV are measured using the experimental setup shown in Fig. 3. Gaussian fitting is performed on the BGS of each fiber and the BFS and Brillouin bandwidth of each fiber are recorded as shown in Fig. 5. For fibers I and II as shown in Figs. 5(a) and 5(b), the BFSs are 16.065 GHz and 16.102 GHz and the BGS bandwidths are 15.54 MHz and 12.31 MHz, respectively. This difference in BFS can be explained by Eq. (9). The difference in dopant concentration between the two fibers results in the differences in the acoustic velocity and the refractive index. This difference in BGS bandwidth is explained as being due to the fact that the increasing of GeO_2 will result in a decrease in phonon lifetime and an increase in bandwidth. Although not each group of fibers is tested at the same length and the same input power, it is clear that the output SBS power is the same, and the product of the fiber length and the input power in the polarization-maintaining fiber is larger, which is the opposite to the influence of germanium concentration on the bandwidth. The results indicate that in LMA fibers with the same core diameter, the BFS decreases and the BGS band-

width increases with the augment of doped germanium concentration in the core. This result is consistent with that of an SMF.[24] The same conclusion is applicable to the fibers III–IV as shown in Figs. 5(c) and 5(d). The BFSs are 16.123 GHz and 16.134 GHz, respectively, and the BGS bandwidths are 15.54 MHz and 12.31 MHz, respectively. The BFS and BGS bandwidth changes of the 10/125 fiber are greater than that of 20/400 fiber. The reason for this result is that the difference in germanium concentration between the two 10/125 fibers is higher than that between the two 20/400 fibers.

The tests of the BGS bandwidth for fibers I–IV are shown in Fig. 1(b), which are compared with the simulations. The diamond, square, circle, and the triangle symbols in Fig. 1(b) indicate the tested BGS bandwidth of the fibers I, II, III, and IV, respectively.

The measured fiber bandwidth is positively correlated with the x-ray signal intensity, and the simulated bandwidth is also proportional to the germanium concentration. That is, as the doped germanium concentration in the core increases, the BGS bandwidth increases. However, there is some obvious departure between the tested value and the simulation one. Besides the fact that the coefficients of Eqs. (4)–(6) are not universal, the germanium concentration used in our fiber is not an absolute concentration but the x-ray signal intensity.

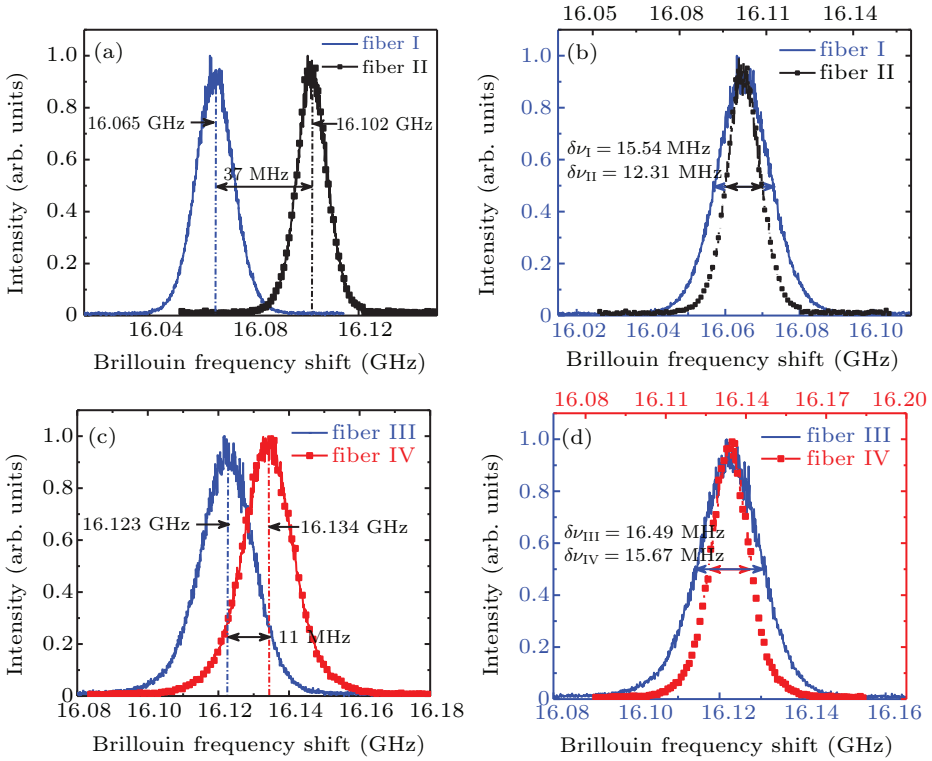


Fig. 5. Comparison of (a) BFS and (b) BGS bandwidth gain spectra between fibers I and II. Comparison of (c) BFS and (d) BGS bandwidth gain spectra between fibers III and IV.

Figure 6(a) shows x-ray signal intensities of GeO_2 doped in the core of three passive optical fibers with different core diameters. The curves represent the x-ray signal intensity distributions in the cross sections of the fibers. The x-ray signal intensity at the core of each fiber is averaged to characterize the core germanium concentration in each fiber. The average x-ray signal intensity in the core of the fibers I, V, and VI are 43.568, 38.17, and 34.17, respectively. Result shows that the small-core fiber has a higher germanium concentration. Figure 6(b) shows the BGS measurement results of three fibers with different core diameters. The lengths of the different fibers range from 20 m to 150 m. We find that the BGSs of three types of fibers all exhibit a Gaussian distribution. The BFS for fibers I, V, and VI are 16.102, 16.138, and 16.168 GHz, respectively, and the BGS bandwidths are 12.31, 14.22, and 15.93 MHz respectively. BGS bandwidth is increased by ~ 2 MHz when the core diameter increases from 10 μm to 30 μm. Fiber I has a higher germanium concentration, but the bandwidth is narrower than that of fiber VI, indicating that the core diameter has a greater effect on the bandwidth than the germanium concentration in the LMA fiber.

We also compare the numerical solution and measured BGS bandwidth of the three fibers with different core diameters, which is shown in Fig. 2(b). It should be noted that single-pass gain G for each fiber is calculated under the condition that the x-ray signal intensity is regarded as the germanium concentration. The circle, square, and triangle symbols indicate the measured BGS bandwidths of fibers I, V, and VI, respectively. The reason for this difference may be that in an LMA fiber, when pump light is coupled into the fiber, multi-

ple conduction transverse modes can be excited. The Stokes light generated by the inelastic collision of the optical photons with the acoustic phonons in the optical fiber also excites multiple conduction modes. The superposition of multiple modes of Stokes light will broaden the BGS bandwidth. Previous literature has reported[33] that the increasing of the number of optical modes can lead the BGS bandwidth to broaden.

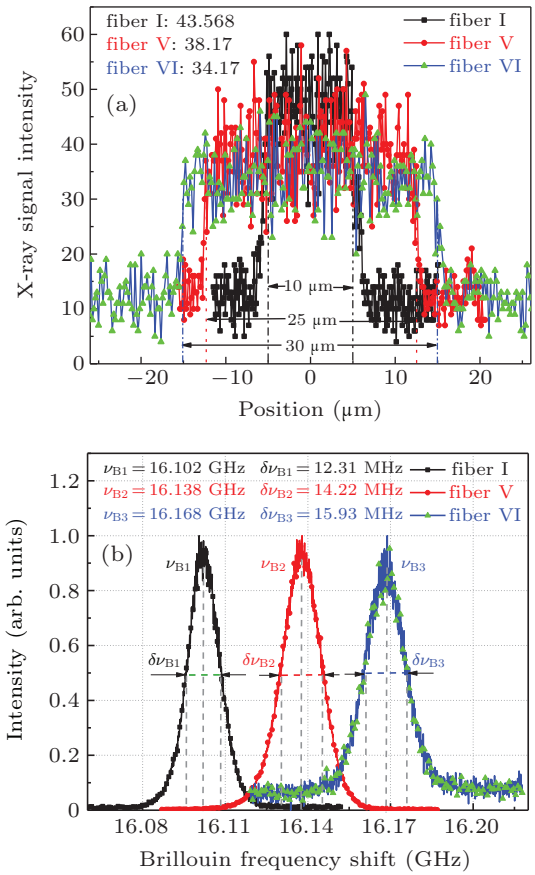


Fig. 6. Comparison among (a) x-ray signal intensities for 10/125, 25/250, and 30/250 fibers and (b) BGSs of fibers for different core diameters.

5. Conclusions

In this work, the dependence of BFS bandwidth and BGS bandwidth on GeO_2 concentration are simulated. It is shown that BGS bandwidth initially increases, then decreases and BFS decreases as the GeO_2 concentration increases. We also provide direct experimental evidence that BFS reduces and the linewidth broadens with the increase of germanium concentration in LMA fiber. Moreover, it is demonstrated experimentally that BGS bandwidth increases as the core diameter increases, and that the BGS bandwidth broadening is because the superposition of multiple transmission modes of Stokes light in LMA fibers causes the entire Brillouin scattering spectrum to broaden. This work will provide reference for multi-wavelength Brillouin lasers.

References

[1] Liu A, Mead R, Vatter T, Henderson A and Stafford R 2004 *Proc. SPIE* **5335** 81
[2] Liu Z J, Zhou P, Wang X J, Wang X L and Ma Y X 2013 *Sci. China* **56** 1597
[3] Richardson D J, Nilsson J and Clarkson W A 2010 *J. Opt. Soc. Am. B* **27** B63
[4] Kobyakov A, Sauer M and Chowdhury D 2009 *Adv. Opt. Photon.* **2** 1
[5] Feng Q S, Cao L H, Liu Z J, Zheng C Y and He X T 2019 *High. Power. Laser. Sci. Eng.* **7** 04000
[6] Zhao X, Yang Y F, Shen H, Chen X L, Bai G, Zhang J P, Qi Y F, He B and Zhou J 2017 *High. Power Laser. Sci. Eng.* **5** E31
[7] Robin C and Dajani I 2011 *Opt. Lett.* **36** 2641
[8] Zhang Z Z, Guo C, Cui L, Zhang Y C, Du C and Li X Y 2019 *Chin. Opt. Lett.* **17** 118
[9] Li M J, Chen X, Wang J, Gray S, Liu A, Demeritt J A, Ruffin A B, Crowley A M, Walton D T and Zenteno L A 2007 *Opt. Express* **15** 8290
[10] Lim K J, Seah S K W, Ye J Y E, Lim W W Y, Seah C P, Tan Y B, Tan S T, Lim H T, Sidharthan R, Prasadh A R, Chang C J, Yoo S and Chua S L 2020 *Photon. Res.* **8** 82
[11] Leigh M, Shi W, Zong J, Yao Z, Jiang S and Peyghambarian N 2008 *Appl. Phys. Lett.* **92** 1326
[12] Anderson B, Flores A, Holten R and Dajani I 2015 *Opt. Express* **23** 27046
[13] Supradeepa V R 2013 *Opt. Express* **21** 4677
[14] Zeringue C, Dajani I, Naderi S, Moore G T and Robin C 2012 *Opt. Express* **20** 21196
[15] Shen H, Lou Q H, Quan Z, Li X W, Yang Y F and Chen X L 2019 *Appl. Opt.* **58** 3053
[16] Gregory D G, Stuart J M, Joshua E R, Timothy S M, Peter A T, Michael G W and Mark E W 2010 *Opt. Lett.* **35** 1542
[17] Zha C W, Peng W J, Wang X J, Wang Y S and Sun Y H 2017 *Opt. Express* **25** 19740
[18] Meng D, Lai W C, He X B, Ma P F, Su R T, Zhou P and Yang L J 2019 *Laser Phys.* **29** aafd24
[19] Wang Y S, Feng Y J, Ma Y, Chang Z and Tang C 2020 *IEEE Photon. J.* **PP** 1
[20] Flores A, Robin C, Lanari A and Dajani I 2014 *Opt. Express* **22** 17735
[21] Harish A V and Nilsson J 2019 *IEEE J Sel. Top. Quantum Electron.* **24** 1
[22] Liu M Z, Yang Y F, Shen H, Zhang J P, Zou X X, Wang H B, Yuan L C, You Y, Bai G and He B 2020 *Sci. Rep.* **10** 629
[23] Anderson B M, Flores A and Dajani I 2017 *Opt. Express* **25** 17671
[24] Nikles M, Thevenaz L and Robert P A 1997 *J. Lightwave. Technol.* **15** 1842
[25] Jiang L, Wang Y, Yang P, Zhang L, Yang L, Dai S and Lou C L 2020 *Opt. Commun.* **459** 125040
[26] Tkach R W, Chraplyvy A R and Derosier R M 1987 *Electron. Lett.* **22** 1011
[27] Mizuno Y and Nakamura K 2010 *Opt. Lett.* **35** 3985
[28] Yeniay A, Delavaux J M P and Toulouse J 2002 *J. Lightwave. Technol.* **20** 1425
[29] Koyamada Y, Sato S, Nakamura S, Sotobayashi H and Chujo W 2004 *J. Lightwave. Technol.* **22** 631
[30] Lü Z W, He W M, Hasi W L J, Zhang Z and Gao W 2008 *Chin. Phys. B* **17** 3765
[31] Boyd R W, Rzazewski K and Narum P 1990 *Phys. Rev. A* **42** 5514
[32] Zhang Y J, Fu X H and Tian Y S 2017 *Acta Phys. Sin.* **66** 024207 (in Chinese)
[33] Minardo A, Bernini R and Zeni L 2014 *Opt. Express* **22** 17480